Aerosol distribution in the Northern Hemisphere during ACE-Asia: Results from global model, satellite observations, and Sun photometer measurements

Mian Chin,[1] Allen Chu,[1,2] Robert Levy,[1,3] Lorraine Remer,[1] Yoram Kaufman,[1] Brent Holben,[4] Tom Eck,[4,5] Paul Ginoux,[6] and Qingxian Gao[7]

Received 27 March 2004; revised 31 August 2004; accepted 21 September 2004; published 2 December 2004.

[1] We analyze the aerosol distribution and composition in the Northern Hemisphere during the Asian Pacific Regional Aerosol Characterization Experiment (ACE-Asia) field experiment in spring 2001. We use the Goddard Chemistry Aerosol Radiation and Transport (GOCART) model in this study, in conjunction with satellite retrieval from the Moderate-Resolution Imaging Spectroradiometer (MODIS) on EOS-Terra satellite and Sun photometer measurements from the worldwide Aerosol Robotic Network (AERONET). Statistical analysis methods including histograms, mean bias, root-mean-square error, correlation coefficients, and skill scores are applied to quantify the differences between the MODIS $1^\circ \times 1^\circ$ gridded data, the daytime average AERONET data, and the daily mean $2^\circ \times 2.5^\circ$ resolution model results. Both MODIS and the model show relatively high aerosol optical thickness (τ) near the source regions of Asia, Europe, and northern Africa, and they agree on major features of the long-range transport of aerosols from their source regions to the neighboring oceans. The τ values from MODIS and from the model have similar probability distributions in the extratropical oceans and in Europe, but MODIS is approximately 2–3 times as high as the model in North/Central America and nearly twice as high in Asia and over the tropical/subtropical oceans. Comparisons with the AERONET measurements in the Northern Hemisphere demonstrate that in general the model and the AERONET data have comparable values and similar probability distributions of τ, whereas MODIS tends to report higher values of τ over land, particularly North/Central America. The MODIS high bias is primarily attributed to the difficulties in land algorithm dealing with surface reflectance over inhomogeneous and bright land surfaces, including mountaintops, arid areas, and areas of snow/ice melting and with land/water mixed pixels. The model estimates that on average, sulfate, carbon, dust, and sea salt comprise 30%, 25%, 32%, and 13%, respectively, of the 550-nm τ in April 2001 in the Northern Hemisphere, with ~46% of the total τ from anthropogenic activities and 66% from fine mode aerosols. *INDEX TERMS:* 0305 Atmospheric Composition and Structure: Aerosols and particles (0345, 4801); 0368 Atmospheric Composition and Structure: Troposphere—constituent transport and chemistry; 0345 Atmospheric Composition and Structure: Pollution—urban and regional (0305); *KEYWORDS:* aerosols, distributions, ACE-Asia

Citation: Chin, M., A. Chu, R. Levy, L. Remer, Y. Kaufman, B. Holben, T. Eck, P. Ginoux, and Q. Gao (2004), Aerosol distribution in the Northern Hemisphere during ACE-Asia: Results from global model, satellite observations, and Sun photometer measurements, *J. Geophys. Res.*, *109*, D23S90, doi:10.1029/2004JD004829.

[1]Laboratory for Atmospheres, NASA Goddard Space Flight Center, Greenbelt, Maryland, USA.
[2]Joint Center for Earth Systems Technology, University of Maryland, Baltimore County, Baltimore, Maryland, USA.
[3]Science System and Applications, Inc., Lanham, Maryland, USA.
[4]Laboratory for Terrestrial Physics, NASA Goddard Space Flight Center, Greenbelt, Maryland, USA.
[5]Goddard Earth Science and Technology Center, University of Maryland, Baltimore County, Baltimore, Maryland, USA.
[6]NOAA Geophysical Fluid Dynamics Laboratory, Princeton, New Jersey, USA.
[7]Chinese Academy of Environmental Science, Beijing, China.

0148-0227/04/2004JD004829$09.00

1. Introduction

[2] The Asian Pacific Regional Aerosol Characterization Experiment (ACE-Asia), which studied the characteristics of aerosols from Asia and their radiative effects, took place in spring 2001 in the western Pacific region near the east coast of Asia. In the spring, dust emission in northern Asia is strong, biomass burning in Southeast Asia is at its peak, photochemical production of pollution aerosols is active, and the continental outflow from Asia to the western Pacific is at its strongest. In other words, the timing of ACE-Asia was optimal for studying the impact of maximum Asian aerosol concentrations on

downwind regions. The ACE-Asia field experiment involved three aircraft and two ships in coordination with surface and lidar networks and satellite overpasses [*Huebert et al.*, 2003]. Coincident to the ACE-Asia observations, which covered only a limited geographical location, measurements from satellites and a world wide, ground-based, Sun photometer network provided global-scale aerosol information. These larger-scale measurements placed the ACE-Asia observations into a broader perspective. A global model can synthesize such a wide array of observations in order to assess the global impact of Asian aerosols and to quantify the processes that control the aerosol composition and distributions.

[3] In this study, we use the Goddard Chemistry Aerosol Radiation and Transport (GOCART) model to address the characteristics of aerosol distribution and composition in the Northern Hemisphere in spring 2001. During the ACE-Asia intensive operation period (30 March to 4 May 2001), the GOCART model was used in the forecast mode, providing daily aerosol forecasts to support the flight planning [*Chin et al.*, 2003; *Huebert et al.*, 2003]. These results have been verified by the aircraft measurements [*Chin et al.*, 2003]. The focus of this paper is to evaluate the model-calculated aerosol optical thickness (τ) and aerosol size information by comparing to the satellite retrieval from the Moderate-Resolution Imaging Spectroradiometer (MODIS) and Sun photometer measurements from the Aerosol Robotic Network (AERONET). The comparisons cover over both source regions and downwind areas in the Northern Hemisphere. Several statistical parameters, including histograms, mean bias, root-mean-square error, correlation coefficients, and skill scores, will be introduced to quantitatively evaluate the model. On the basis of the model results, we estimate the aerosol composition and the anthropogenic contributions in the Northern Hemisphere during spring 2001. The present work leads to a companion paper (M. Chin et al., Intercontinental transport of aerosols in the context of ACE-Asia, manuscript in preparation, 2004), which specifically addresses the impact of long-range transport of pollution and dust aerosols originating from major source regions on regional and hemispheric scales.

[4] Section 2 provides a short description of the GOCART model and the MODIS and AERONET measurements. In section 3, we first compare the distributions of τ and the fraction of fine mode aerosols (f_τ) calculated from the model with those retrieved from the MODIS instrument. Then we use the measured τ from 57 AERONET Sun photometer sites in the Northern Hemisphere to evaluate the corresponding quantities from MODIS and the model. In section 4, we estimate the aerosol composition and fractions of anthropogenic versus fine mode aerosols in total τ. We discuss the results and possible causes of discrepancies between the model and observations in section 5 before we conclude in section 6.

2. Description of the Model and the Data

2.1. GOCART Model for Tropospheric Aerosols

[5] Detailed description of the GOCART model has been presented and results have been extensively evaluated in our previous publications [*Chin et al.*, 2000a, 2000b, 2002, 2003; *Ginoux et al.*, 2001, 2004]. Here we provide a brief summary of the GOCART model and its recent modifications. The model simulates major tropospheric aerosol types of sulfate, dust, organic carbon (OC), black carbon (BC), and sea salt. It uses assimilated meteorological fields from the Goddard Earth Observing System Data Assimilation System (GEOS DAS) that include winds, temperature, pressure, specific and relative humidity, cloud mass flux, cloud fraction, precipitation, boundary layer depth, surface winds, and surface wetness. The spatial resolution of the model is currently at 2° latitude by 2.5° longitude, with total 30 vertical layers. Physical processes in the model include emission, advection, convection, boundary layer mixing, wet deposition (rainout and washout), dry deposition (a function of surface resistance and atmospheric stability), and gravitational settling. Chemical processes include gas and aqueous phase reactions that convert sulfate precursors (dimethylsulfide, or DMS, and SO_2) to sulfate.

[6] Global emissions of aerosols and their precursors have been updated and modified from the earlier version of the GOCART simulations [*Chin et al.*, 2002, 2003] to reflect the most recent knowledge about these sources. Anthropogenic emissions of SO_2, OC, and BC for Asia are from the most recent and detailed emission inventory for the year 2000 [*Streets et al.*, 2003]. For the rest of the world, we use the IPCC emission scenario of SO_2 for 2000 [*Nakićenović et al.*, 2000]. Biomass-burning emissions of SO_2, OC, and BC for March and April 2001 are obtained on the basis of the CO emissions estimated from the AVHRR satellite fire counts [*Heald et al.*, 2003] and the burned biomass inventory constructed using other satellite data [*Duncan et al.*, 2003; *Chin et al.*, 2002].

[7] The dust sources are assumed to be in topographic depression areas with bare soil surfaces, and the dust uplifting probability is defined according to the degree of depression [*Ginoux et al.*, 2001]. Over Asia, the dust source is modified to include the detailed surface information and the recent desertification regions over China (Q. Gao, unpublished data, 2002), which seem to be mainly responsible for the boundary layer dust over the western Pacific observed during ACE-Asia [*Chin et al.*, 2003]. Dust particles ranging from 0.1 to 10 μm in radius are simulated by the model.

[8] Volcanic emissions take account of sources from both continuously and sporadically erupting volcanoes. The major source of volcanic emissions in the ACE-Asia region is the Miyakejima volcano in Japan (34.08°N, 139.53°E), which started erupting in September 2000. The Miyakejima volcanic plume was estimated to have reached 500–2000 m above the rim, emitting 20–50 kt SO_2/d (e.g., http://hakone.eri.u-tokyo.ac.jp/vrc/erup/miyake.html). Here we assume an emission rate of 28 kt SO_2/d from January to mid-May 2001 with an emission height at 1500 m above the volcanic rim (813 m above sea level).

[9] Other emissions in the model include biogenic emissions of OC and oceanic emissions of DMS and sea salt (0.1–10 μm), which have been described previously [*Chin et al.*, 2002, 2003]. Figure 1 shows the emissions in April 2001 of sulfur (SO_2, DMS, and sulfate), carbonaceous (OC + BC), dust, and sea-salt emissions for the Northern Hemisphere in this study.

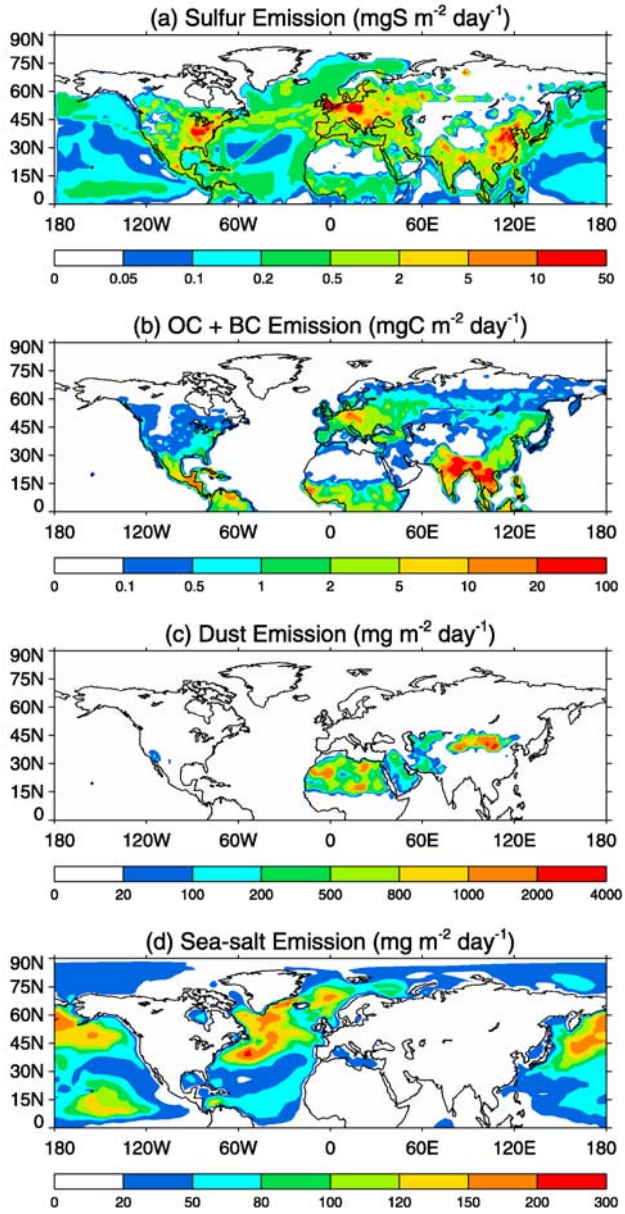

Figure 1. Emissions of (a) sulfur (SO_2, DMS, and sulfate), (b) carbon (OC and BC), (c) dust, and (d) sea salt in the Northern Hemisphere in April 2001 used in the model.

[10] The aerosol optical thickness τ is determined from the dry mass concentrations and the mass extinction coefficients. The mass extinction coefficients are calculated from the Mie theory on the basis of size distributions, refractive indices, and hygroscopic properties of individual aerosol types. We assume single-mode lognormal size distributions for sulfate, OC, and BC aerosols as well as for each dust and sea-salt size bins (details given by *Chin et al.* [2002]). Although a recent study has shown that the difference of extinction coefficient between externally and internally mixed aerosols is between 0 to over 50% (internal mixture being lower) depending on the relative humidity and aerosol composition [*Lesins et al.*, 2002], we assume here that all aerosol particles are externally mixed because of the difficulties in realistically determining the degree of the mixing state.

2.2. Aerosol Data From MODIS Retrievals and AERONET Measurements

[11] The MODIS instrument aboard the EOS-Terra satellite, which has been taking aerosol measurements since 2000, provides daily nearly global coverage with local equatorial overpass time about 10:30 am [*King et al.*, 1999]. The MODIS aerosol retrieval uses separate algorithms over land and ocean to obtain aerosol optical properties in cloud free areas, including total aerosol optical thickness τ and fine mode (submicron particle size) aerosol fraction f_τ [*Tanré et al.*, 1997; *Kaufman et al.*, 1997a, 2002; *Remer et al.*, 2002, 2004; *Chu et al.*, 1998, 2002, 2003; *Levy et al.*, 2003, 2004]. We use in this study the version 4 level-3 quality-assured MODIS daily τ at 550 nm, which is a globally gridded data set at $1^\circ \times 1^\circ$ horizontal resolution. There is no aerosol retrieval over bright land surfaces (such as desert and snow covered surfaces) and ocean sun glint areas.

[12] Over ocean, the τ in seven wavelength bands (0.47–2.13 μm) and f_τ are retrieved by a "least residual method" that minimizes the difference between measured and calculated reflectance at the top of atmosphere. The calculated reflectance is obtained from optimized combinations of four fine and five coarse aerosol property lognormal modes [*Tanré et al.*, 1997]. Over land, the aerosol properties are derived in two visible wavelengths (0.47 and 0.66 μm) using the "dark target" method that assumes a globally fixed empirical ratio between the surface reflectance in the two visible wavelengths to the measured reflectance at 2.13 μm ($R_{0.47}/R_{2.13}$ = 0.25, $R_{0.66}/R_{2.13}$ = 0.50) [*Kaufman et al.*, 1997b]. The path radiance is determined to be a function of the difference between the estimated surface reflectance and the satellite-measured reflectance in the two visible channels. The fine mode fraction f_τ over land in the MODIS standard product is obtained on the basis of the ratio of the path radiance in the two visible wavelengths, a relatively narrow spectral range that may cause high bias of f_τ [*Chu et al.*, 2003]. In this study, we use an alternative formulation of f_τ that reduces the high bias of f_τ over land. Here, the land f_τ is determined from the Ångstrom exponent (α) over land and the knowledge of the relationship of f_τ and α over ocean (D. A. Chu et al., Characterization of aerosol properties by MODIS during ACE-Asia experiment, submitted to *Journal of Geophysical Research,* 2004), thus taking advantage of more accurate ocean retrievals obtained using a wider spectral range (0.47–2.13 μm). Even with improved formulation of f_τ, retrievals of τ still have large uncertainties, because the assumption of the empirical surface reflectance ratios seems too simple to account for the complexities of land surface reflectance [*Levy et al.*, 2004].

[13] The AERONET, an international federated Sun photometer network [*Holben et al.*, 1998], currently has about 180 ground-based remote sensing monitoring stations. These sites represent virtually all aerosol regimes in a wide range of geographic locations, through seasonal and annual cycles. AERONET measures the total column aerosol spectral optical thickness at several visible and near infrared wavelengths, and derives a number of column-representative aerosol properties, including total and absorbing τ, size

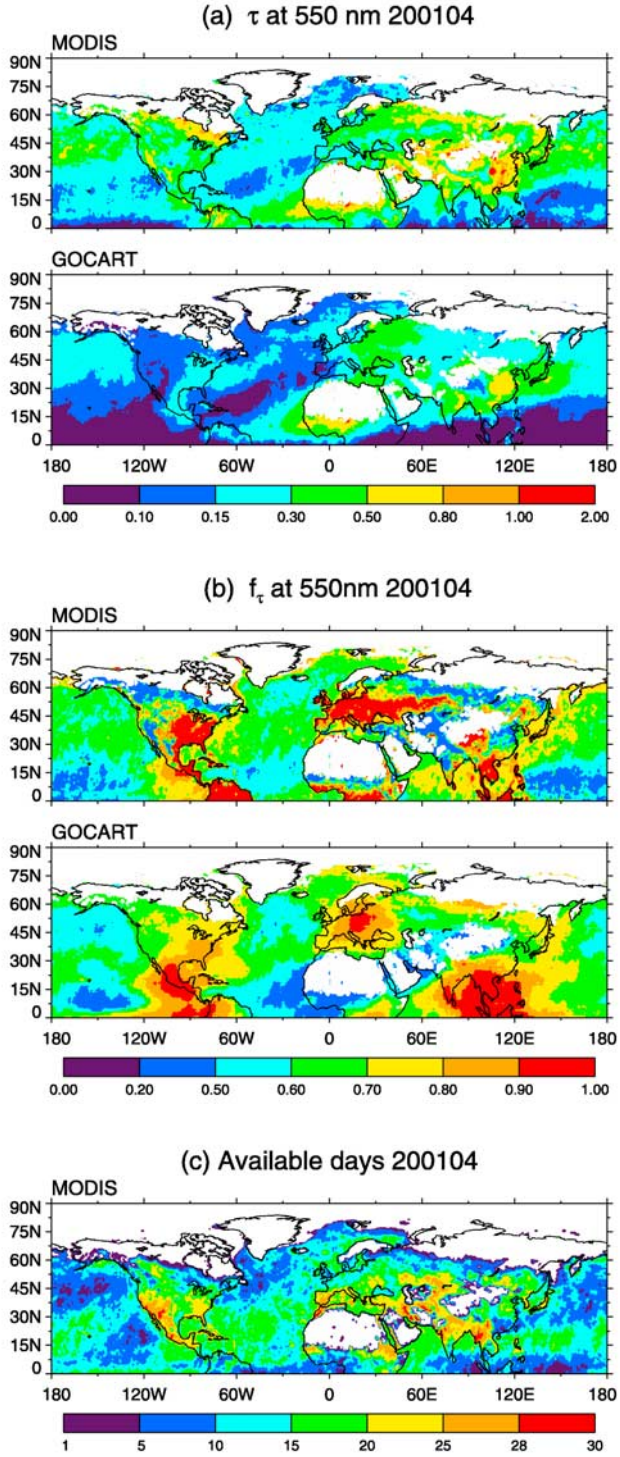

Figure 2. Northern hemispheric distributions of (a) 550-nm aerosol optical thickness (τ) and (b) fine model fraction (f_τ) from the MODIS and the model for April 2001, averaged over the locations and days that MODIS measurements are available, which are shown in Figure 2c.

distribution, single-scattering albedo, and complex index of refraction [*Holben et al.*, 1998, 2001; *Eck et al.*, 1999; *Dubovik et al.*, 2002]. The accuracy of τ in the AERONET field instruments is $\sim$0.01–0.02 [*Eck et al.*, 1999]. Since they are from direct measurements, AERONET data are considered to be the "ground truth" for satellite and model validations [e.g., *Remer et al.*, 2002; *Chu et al.*, 2002; *Chin et al.*, 2002]. Like satellite data, however, Sun photometer acquires aerosol data only during daylight in cloud free conditions. We use the quality-assured and cloud-screened level-2 AERONET data [*Smirnov et al.*, 2000].

3. Aerosol Distribution During ACE-Asia: Comparisons Between the Model and Observations

[14] There are spatial and temporal sampling differences among MODIS and AERONET data, both of which are subsets of the model. The model results are daily (24-hour) averages at 2° latitude × 2.5° longitude spatial resolution, while the AERONET data are daytime average at specific site locations and the MODIS retrievals are "instantaneous" at a local overpass time of 10:30 am with 1° × 1° spatial resolution. In addition, the model results are for both cloudy and clear sky conditions, whereas the AERONET and MODIS data represent only clear sky conditions. This means that some differences among these results should be expected even in the most ideal situation (e.g., no error from measurements, retrievals or model). We compare the τ values at a commonly referred wavelength of 550 nm. Since the 550 nm τ is not directly measured by AERONET, it is interpolated from the 440 nm and 670 nm AERONET data assuming linear relationships between log wavelength and log τ.

[15] We use a number of statistical parameters to evaluate the quality of the model output, which we refer to as "*HERBS*": The histogram (*H*), which shows similarity between the peak, spread, and skewness of the observed and calculated aerosol distributions; the root-mean-square error (*E*), which reveals the magnitude of absolute difference between the model and observations; the correlation coefficient (*R*), which measures the linear correspondence; and the mean bias (*B*), which represents the ratio of the model results to the data. The skill score (*S*), which considers both correlation and standard deviation between two data sets, is defined as

$$S = \frac{4(1+R)}{\left(\sigma_f + 1/\sigma_f\right)^2 (1+R_0)},$$

where σ_f is the ratio of the standard deviations of two data sets, and R_0 is the maximum attainable correlation coefficient [*Taylor*, 2001]. Here, we assume R_0 to be 1, although in reality it should always be less than 1 because of some intrinsic differences (e.g., spatial and time resolution) between the model and observations. The *S* value ranges from 0 to 1.

3.1. Aerosol Distribution in the Northern Hemisphere in Spring 2001

[16] Monthly averaged northern hemispheric distributions of τ and fine mode fraction f_τ from MODIS and the model in April 2001 are shown in Figures 2a and 2b, respectively. The f_τ from the model is defined as the ratio of the sum of the τ from sulfate, OC, BC, and submicron dust and sea salt to the total τ. As we mentioned in section 2, MODIS is unable to retrieve aerosol information over bright surfaces, in the presence of clouds, and over ocean sun glint areas,

therefore with fewer observational days over ocean than over land because of more frequent cloud cover and sun glint interference. Also, there is no data over large desert areas in Sahara, Arabia, and Asia and most of the areas north of 60°N (Figure 2c). The monthly averaged results from the model in Figures 2a and 2b are constructed from the daily values that match the days and locations of the available MODIS data (Figure 2c) for a more meaningful comparison.

[17] Both MODIS and the model show relatively high τ near the source regions such as eastern Asia, Europe, and northern Africa. They also reveal some major features of the long-range transport, such as from Asia to North Pacific, from North America to North Atlantic, and from Africa to the equatorial North Atlantic (Figure 2a). The most noticeable differences occur in North America and in the subtropical/tropical oceans, where the τ from MODIS is a factor of 2–3 higher than those from the model. We will discuss these discrepancies later.

[18] When the monthly averaged f_τ for April 2001 from MODIS and the model are compared (Figure 2b), both show that f_τ is greater than 0.5 over most areas in the Northern Hemisphere with the highest values (>0.8) in and near the anthropogenic and biomass-burning source regions. However, the f_τ from MODIS is 0.1 to 0.5 higher than the model in the eastern United States, Europe, and equatorial Africa, and is 0.3 to 0.5 lower than the model at high latitudes (about 60°N) over land (North America and Eurasia) and over the equatorial Pacific and Indian oceans. In addition, the MODIS f_τ data also show discontinuities at some land-ocean borders, presumably from the use of different retrieval algorithms for land and ocean.

[19] To further analyze the similarities and differences in spatial distributions between the MODIS and the model, we plot in Figure 3 the probability distributions (or normalized histograms) of τ and f_τ at different land and oceanic regions in the Northern Hemisphere. Here, the western North Pacific, eastern North Pacific, and North Atlantic oceans are divided into northern (latitude $\geq$ 30°N) and southern (latitude < 30°N) parts, with a total of six oceanic subregions. The land is also divided into six subregions: Northern and southern Asia, northern and southern America, Europe, and Africa/Middle East, all separated by the 37°N latitudinal line.

[20] The τ values from MODIS and the model have similar distributions (close to lognormal) over the northern part of North Pacific and North Atlantic oceans where the most probable, or modal, τ (τ_m) is about 0.2–0.3, with the model being 25 to 33% lower (Figure 3a, left column). In the southern parts, however, they differ by almost a factor of 2; the τ_m in the model is 0.08–0.11 whereas MODIS reports 0.15–0.2 (Figure 3a, right column). These differences are consistent with Figure 2. Over land (Figure 3b), the model displays similar τ_m distributions to MODIS in Europe (τ_m at 0.36), but are significantly lower than MODIS for other regions. The largest discrepancy is clearly over North America where the τ_m from the model (0.11) is less than a third of MODIS (0.36).

[21] Figures 3c and 3d show the probability distributions of f_τ over the same ocean and land subregions that are displayed Figures 3a and 3b. Both MODIS and the model show similar normal distributions over the oceanic regions, except in the southern NW and NE Pacific where the model indicates a second peak at f_τ of 0.9 where MODIS has only a single peak at 0.5 (Figure 3c). Over land, MODIS exhibits a relatively constant distribution of f_τ, between 0.2 and 1, in northern Asia and northern North America, whereas the model displays a well-defined symmetrical distribution with a modal f_τ of 0.68. In other land regions, the MODIS data indicate that aerosols are predominantly composed of small particles with a modal $f_\tau >$ 0.9. The model agrees with MODIS in southern Asia but shows considerably lower f_τ (differences between 0.12 and 0.47) in other areas (Figure 3d).

[22] The regions where MODIS and the model have the largest discrepancies include North/Central America, northern Asia, and tropical/subtropical oceans, where the model values are less than one half of those from MODIS. In other areas, the model agrees with MODIS reasonably well, although the τ from the model is generally lower than that from MODIS. These differences are further analyzed in the next section, by including AERONET data.

3.2. Daily Variations of Aerosols

[23] The daily variations of τ from the model calculations and from the MODIS retrievals are compared with that measured by the AERONET Sun photometers. There are 57 AERONET sites in the Northern Hemisphere that have at least 3 days of measurements during April 2001. These sites include in anthropogenic and dust source regions of Asia, North America, Europe, Africa, and Middle East, oceanic regions immediately downwind of aerosol sources, and cleaner locations in the tropical oceans. Locations of the 57 sites are listed in Table 1 and are also shown in Figure 4 superimposed with the modeled monthly average τ for April 2001. (We will use the site numbers in Table 1 to facilitate our discussions throughout the text.) No MODIS data are available at sites 1–2 in the Asian dust area and 48–49 in the Arabian Desert, because of their very bright surfaces.

[24] Figure 5 shows the time series of daily τ in April 2001 from AERONET, MODIS, and the model at a subset of the AERONET sites. There are three sites each in Asia (first row), North America (second row), Europe/Africa (third row), and oceans (last row), demonstrating daily variability seen in these geographic regions.

[25] In Asia, Beijing (site 4) has high local pollution sources all year long but is heavily under the influence of dust in springtime. Large aerosol episodes observed by AERONET on 4, 8, 10, 18, and 28 April are mostly associated with dust events. Here the model-calculated τ is about half of that measured by AERONET, even though the temporal variations from the model are similar to those of AERONET. At Je-Ju Island of South Korea (site 6) and Shirahama of Japan (site 8), the model indicates that pollution aerosols (mostly sulfate) contribute almost 60–70% to the total τ. These two sites also receive large amount of dust in spring, where 40% and 30% of τ at Je-Ju and Shirahama, respectively, are from dust that has been transported from the Asian continent. The observed large dust peaks on 13 April at Je-Ju and on 14 April at Shirahama are successfully captured by the model. The model predicts a sulfate insurgence on 18 April at Shirahama from the nearby Miyakajima volcano, but there are no available AERONET or MODIS data to verify the model results.

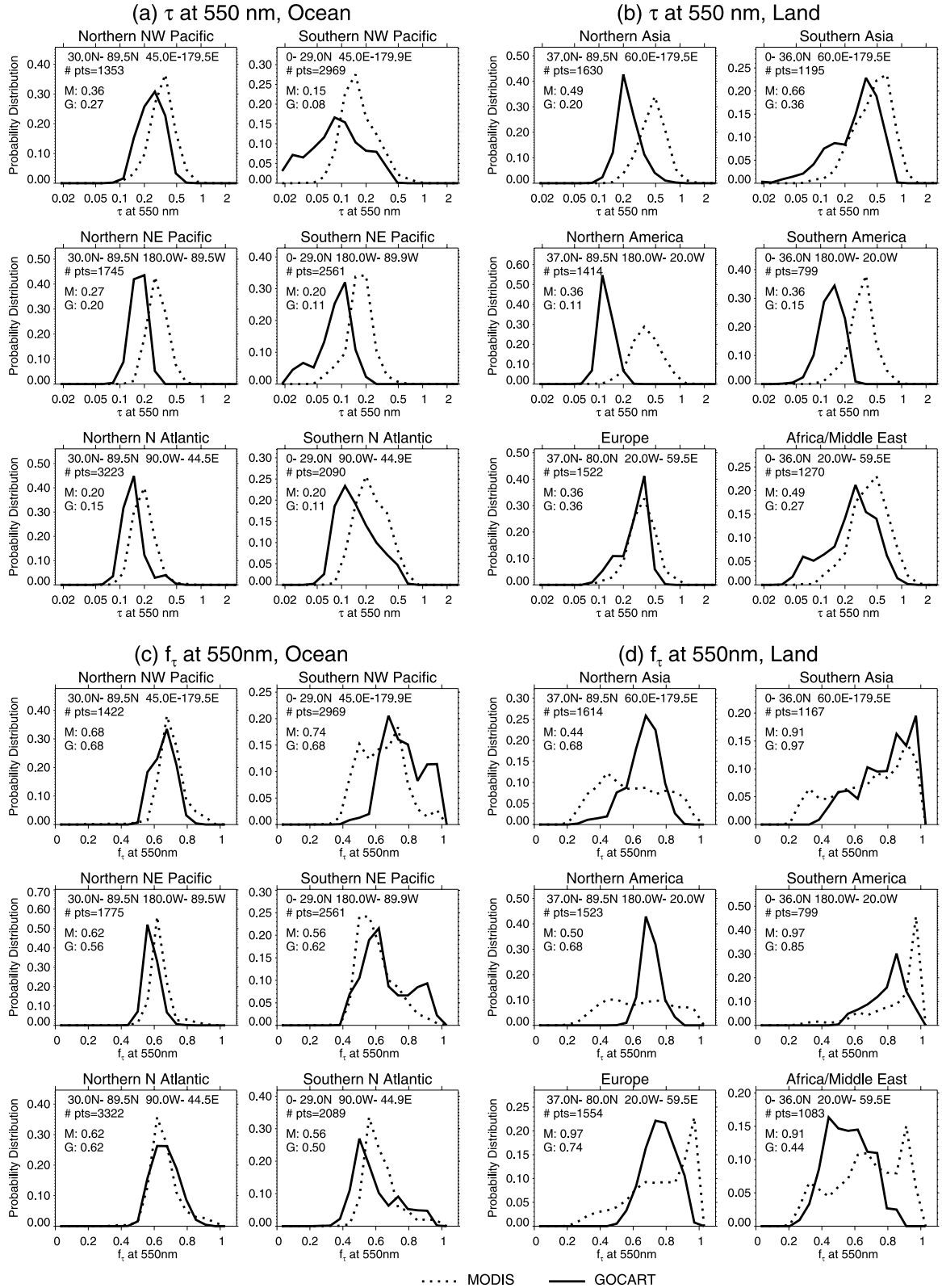

Figure 3. Probability distribution of MODIS (dotted lines) and model (solid lines) products of aerosol optical thickness τ over (a) ocean and (b) land, and the fine mode fraction f_τ over (c) ocean and (d) land. The latitude and longitude borders for each subregion are indicated in each panel. The most probable (or modal) values of MODIS (M) and GOCART (G) for each region are shown in the corresponding panel.

Table 1. Site Number, Name, Location, and Principal Investigator of the 57 AERONET Sites

	Site Name	Latitude	Longitude	Principal Investigator
		Asia		
1	Dunhuang	40.04°N	94.79°E	B. Holben
2	Inner Mongolia	42.68°N	115.95°E	B. Holben
3	Dalanzadgad	43.58°N	104.42°E	B. Holben
4	Beijing	39.98°N	116.38°E	P. Gouloub/H. Chen
5	XiangHe	39.75°N	116.96°E	B. Holben
6	Je-Ju	33.28°N	126.17°E	B. Holben
7	Anmyon	36.52°N	126.32°E	B. Holben/C. McClain
8	Shirahama	33.69°N	135.36°E	B. Holben
9	Noto	37.33°N	137.14°E	I. Sano
10	Taiwan	24.90°N	121.10°E	G.-R. Liu
11	Okinawa	26.36°N	127.77°E	B. Holben
12	Kanpur	26.45°N	80.35°E	B. Holben/R. Singh
		America		
13	Saturn Island	48.78°N	123.13°W	N. O'Neill
14	Rimrock	46.49°N	116.99°W	B. Holben
15	Missoula	46.92°N	114.08°W	W.-M. Hao
16	San Nicolas	33.26°N	119.49°W	R. Frouin
17	Rogers Dry Lake	34.93°N	117.89°W	J. Vandenbosch
18	La Jolla	32.87°N	117.25°W	R. Frouin
19	Maricopa	33.07°N	111.97°W	B. Holben
20	Tucson	32.23°N	110.95°W	K. Thome
21	Sevilleta	34.35°N	106.89°W	D. Moore
22	Cart Site	36.61°N	97.41°W	M. J. Bartholomew
23	KONZA_EDC	39.10°N	96.61°W	D. Meyer
24	Bondville	40.05°N	88.37°W	B. Holben
25	Walker Branch	35.96°N	84.29°W	B. Holben
26	GSFC	39.03°N	76.88°W	B. Holben
27	MD Science Center	39.28°N	76.62°W	B. Holben
28	COVE	36.90°N	75.71°W	B. Holben
29	Egbert	44.23°N	79.75°W	N. O'Neill
30	CARTEL	45.38°N	71.93°W	A. Royer/N. O'Neill
31	Howland	45.20°N	68.73°W	B. Holben
32	Stennis	30.37°N	89.62°W	D. Noel
33	Dry Tortugas	24.60°N	82.80°W	K. J. Voss
34	Mexico City	19.33°N	99.18°W	B. Holben
35	Surinam	5.80°N	55.20°W	B. Holben
		Europe		
36	Avignon	43.93°N	4.88°E	M. Verbrugghe
37	IMC Oristano	39.91°N	8.50°E	D. Tanré
38	Ispra	45.80°N	8.63°E	G. Zibordi
39	Venice	45.31°N	12.51°E	G. Zibordi
40	Rome Tor Vergata	41.84°N	12.65°E	G. P. Gobbi
41	SMHI	58.58°N	16.15°E	B. Hakansson
42	Bucharest	44.45°N	26.52°E	D. Tanré
		Africa		
43	Ouagadougou	12.20°N	1.40°W	D. Tanré
44	Ilorin	8.32°N	4.34°E	R. T. Pinker
45	THALA	35.55°N	8.68°E	B. Holben
		Middle East		
46	IMS-METU-ERDEMLI	36.56°N	34.26°E	B. Holben
47	Nes Ziona	31.92°N	34.79°E	B. Holben
48	Sede Boker	30.52°N	34.47°E	B. Holben
49	Solar Village	24.91°N	46.41°E	B. Holben
		Ocean		
50	Midway Island	28.21°N	177.38°W	B. Holben
51	Coconut Island	21.43°N	157.79°W	C. McClain
52	Lanai	20.74°N	156.92°W	C. McClain
53	La Paguera	17.97°N	67.04°W	B. Holben
54	Bermuda	32.37°N	64.70°W	B. Holben
55	Azores	38.53°N	28.63°W	B. Holben
56	Cape Verde	16.73°N	22.93°W	D. Tanré
57	Male	4.19°N	73.53°E	B. Holben

[26] In North America (second row, Figure 5), Missoula (site 15) in the western United States is proximate to dust transported from Asia during the spring season, KONZA_EDC (site 23) in the central United States (Kansas) is influenced by both local sources and transport, whereas GSFC (site 26) in the eastern United States is dominated by pollution and sulfate aerosols. As shown in Figure 5, sulfate amount increases whereas dust decreases eastward across North America. Yet, the Asian dust can arrive to east coast of North America, suggested by the model. About 15% of the τ at GSFC during April is dust, most which is transported from Asia. At Missoula, model estimates of τ are similar to AERONET, about half of the values retrieved by MODIS. The high values of MODIS may be attributed to the complexity of Missoula's land surface; which is arid and surrounded by mountains and snow. At KONZA_EDC, both AERONET and MODIS show a large episode on 13 April that is not reproduced by the model.

[27] Avignon (site 36) is located near the coast in southern France where both the model and AERONET usually report τ as below 0.2. The τ from MODIS, on the other hand, is nearly double that from both AERONET and the model. The high values from MODIS are related to the coastal nature of the site with mixed land/water pixels, leading to a high bias [*Chu et al.*, 2002]. The large dust event on 21 April over Bucharest (site 42 in Romania) is indicated by both the model and the AERONET data (no MODIS data on that day), although the τ from the model is 50% higher than that from AERONET. It appears that this dust was transported from Africa, where a similar maximum occurred 1–2 days earlier at THALA (site 45 in Tunisia) detected by both measurements and the model. During the last 5 days in April, the model simulates a large dust episode at THALA, which is consistent with MODIS observations. The τ values, however, are more than double those of AERONET.

[28] The effects of land surface properties on the MODIS retrieval quality are reflected in the results at Bucharest (site 42) and Missoula (site 15, in the United States). Although they are located at similar latitudes, Bucharest, elevation at 44 m, was snow free in early April 2001, where the MODIS retrieval agrees with the AERONET data within 25%; by contrast, Missoula, at 1028 m altitude and surrounded by mountains, had snow on the surface in April, where MODIS overestimates the τ by more than a factor of 2.

[29] At three oceanic sites, Midway (site 50) in the open Pacific Ocean, Bermuda (site 54) and Azores (site 55) in the western and eastern North Atlantic, the model shows a sea-salt contribution of 13–19% to the total τ in April 2001. The model indicates that dust is the most important aerosol component at both Midway and Azores (35%), originating from either Asia or from northern Africa, whereas the pollution sulfate from North America contributes to about 50% of total τ at Bermuda.

3.3. Statistical Analysis of Aerosol Optical Thickness at AERONET Sites

[30] We grouped the 57 AERONET sites into four geographic regions in order to perform statistical analysis. Of those sites, 12 are in Asia, 23 in North America plus Surinam (we use "America" for this region), 14 are in Europe/Africa/Middle East, and 8 are in the islands over the

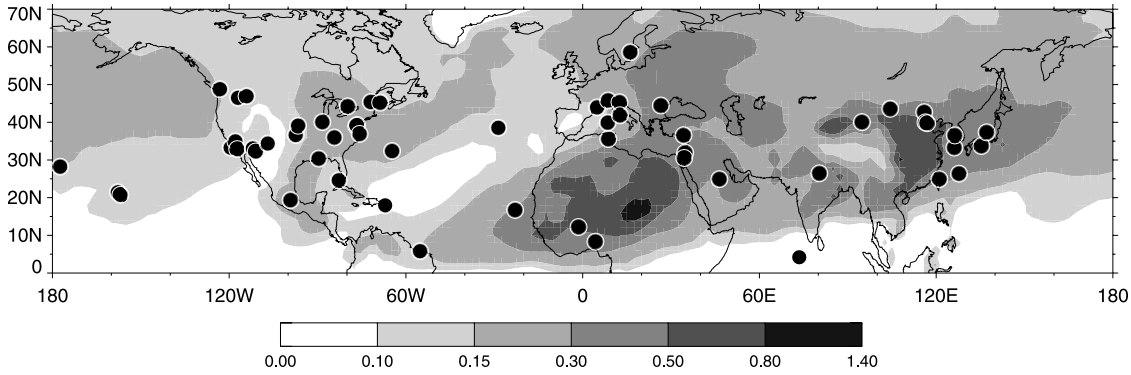

Figure 4. Locations of 57 AERONET sites in the Northern Hemisphere with >3 days of measurements available during April 2001 (see Table 1 for details). Superimposed is the model-calculated monthly average τ at 550 nm for April 2001.

oceans (Table 1). The statistical parameters of mean bias (B), root-mean-square error (E), correlation coefficient (R), and skill score (S), between the model and observations for the 57 sites are summarized in Figure 6. Only days in April 2001 when either AERONET or MODIS data are available are analyzed (days shown in the last panel of Figure 6). While the B (first panel) measures the magnitudes of the model results relative to the data, the E (second panel) points out the absolute differences that are generally proportional to the magnitude of the τ. The model shows relatively large differences (ranging between one half and double) as compared to AERONET data at the Asian dust sites Dunhuang (site 1) and Dalanzadgad (site 3) and also the immediate downwind sites Beijing and Xianghe (sites 4 and 5). This finding illustrates the challenge in modeling the large spatial and temporal variability of dust near its source by a relatively coarse resolution model. Similar to the results shown in Figures 2 and 3, the model reports τ values much lower than by MODIS, ranging between a factor of 2–4. As compared to AERONET, however, model has relatively small errors and biases (mostly within 50%). At several sites in Africa and the Middle East (sites 43–46), the model agrees better with MODIS than with AERONET. Over the ocean, the model agrees with AERONET to within 50% at all sites, except at Male (site 57), but consistently reports much lower values (50–120%) than MODIS. At Male, located near the tropics, has the lowest τ among 8 oceanic sites shown in Figure 4. Here the modeled April averaged τ (0.03) is much lower than both AERONET and MODIS data, with a mean bias $B = 0.3$.

[31] The correlation coefficient R (third panel in Figure 6) reflects the model's performance at simulating the observed daily variation of τ. The R varies from -0.23 to 0.96 between the model and AERONET and -0.20 to 0.92 between the model and the MODIS. These two sets of R usually track each other with a few exceptions, such as Rodgers Dry Lake in the Southwest United States (site 17) and two African sites of Ouagadougou (site 43) and Ilorin (site 44). At Rodgers Dry Lake, the R is 0.7 between the model and AERONET but -0.1 between the model and MODIS; note that the τ from the model is 4 times lower than MODIS but about the same as AERONET. In contrast, the R values between the model and MODIS at Ouagadougou and Ilorin are 0.92 and 0.70, respectively, but the model is negatively correlated to AERONET at these two sites ($R = -0.05$). This may be attributed to the fact that MODIS has far fewer days of coverage than AERONET (last panel in Figure 6) missing some extreme cases, particularly at Ilorin. The skill score (S) offers a more comprehensive assessment of the model performance than other parameters of B, E, and R, because it considers both correlation and variance between the model and the data. As shown in the fourth panel of Figure 6, whereas the model indicates comparable skills in simulating the AERONET and MODIS data in Asia, Europe, and Middle East, it is much more skillful in reproducing the AERONET data than MODIS at almost every site in North America and over oceans.

[32] The probability distributions of the daily τ at sites in each geographic region are shown in Figure 7. Days included in the histograms are those when both MODIS and AERONET measurements are available, so that some of the dust sites are not included here for lack of MODIS retrievals. The model results for the matching dates are also plotted. The τ typically exhibits a probability distribution that is approximately lognormal, as shown previously from AERONET observations [*O'Neill et al.*, 2000]. Over Asia (Figure 7a), the model and AERONET have similar distributions with the modal value, τ_m, at 0.35. The shape of the MODIS distribution is somewhat skewed toward high τ, with a τ_m at 0.64. In America (Figure 7b), the model and AERONET have a similar τ_m at 0.13, with AERONET showing a wider range. The τ values from MODIS in this region are, as seen before, considerably higher than both AERONET and the model, with a τ_m at 0.27. In Europe/Africa/Middle East region (Figure 7c), we find the τ_m of the model (0.23) in between MODIS (0.32) and AERONET (0.16). Over the 8 oceanic sites (Figure 7d), the AERONET, MODIS, and model all illustrate a bimodal distribution, but the model and AERONET have a dominant peak with τ_m of 0.13 whereas the MODIS shows equal magnitude between the two modes.

[33] Figure 8 summarizes the monthly averaged τ for April 2001 from AERONET, MODIS, and the model at the 57 AERONET sites, obtained by averaging only the days with available observations from both AERONET and MODIS. The exceptions are the dust sites 1–2 and 48–49 where only AERONET and the model are available. The statistical parameters B, E, R, and S for each region are listed in Figure 8. The AERONET data can be considered as "calibration reference" because they are from direct mea-

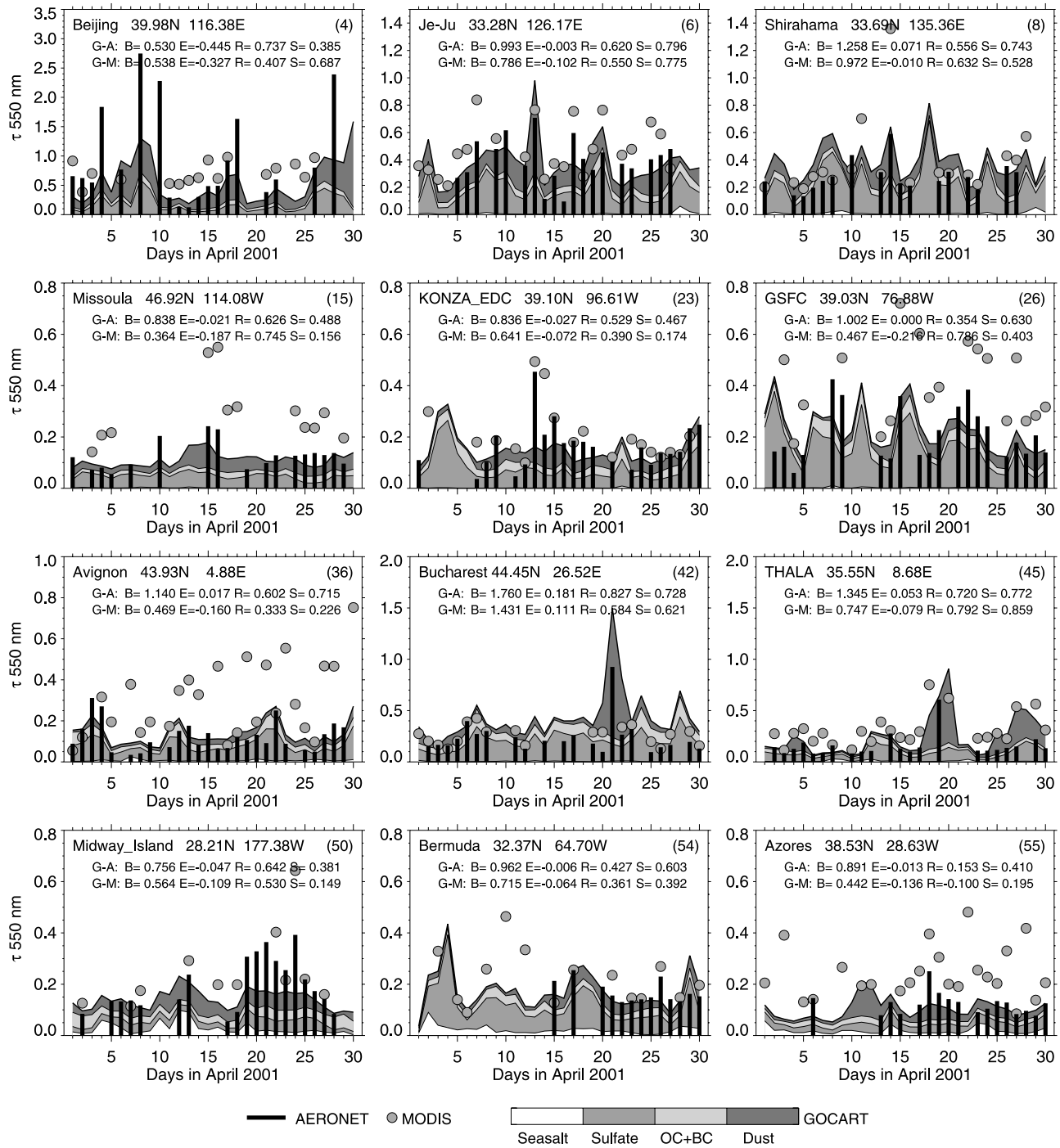

Figure 5. Daily τ at 550 nm from AERONET, MODIS, and the model at 12 AERONET sites in April 2001. Vertical bars, AERONET data; grey circles, MODIS data; lines and shaded areas, GOCART model results with aerosol compositions. Statistical parameters of mean bias (B), root-mean-square error (E), correlation coefficient (R), and skill score (S) between the GOCART model and AERONET (G-A) or GOCART and MODIS (G-M) are listed in each panel.

surements of high accuracy, even though their data may not always be representative of the 100–200 km grid area in the MODIS or model results. Figure 8 clearly shows the τ values from MODIS at most sites in America that are significantly higher than both AERONET and the model, especially from sites 17 and 19–21 located in the Southwest United States and sites 29–31 at high latitudes in northeast of North America. MODIS differences for these sites may be attributed to the complexity of the land surfaces, including: snow/ice melting during spring in high-latitude regions, mixed land/water surface subpixels at coastal or swamp sites, and high surface albedo at mountaintop and arid areas. The model agrees with AERONET within a factor of 2 at all sites except for Dunhuang (site 1), Taiwan (site 10), and Male (site 57), where it differs from AERONET by a factor of 3. Assuming the AERONET data to be a reference

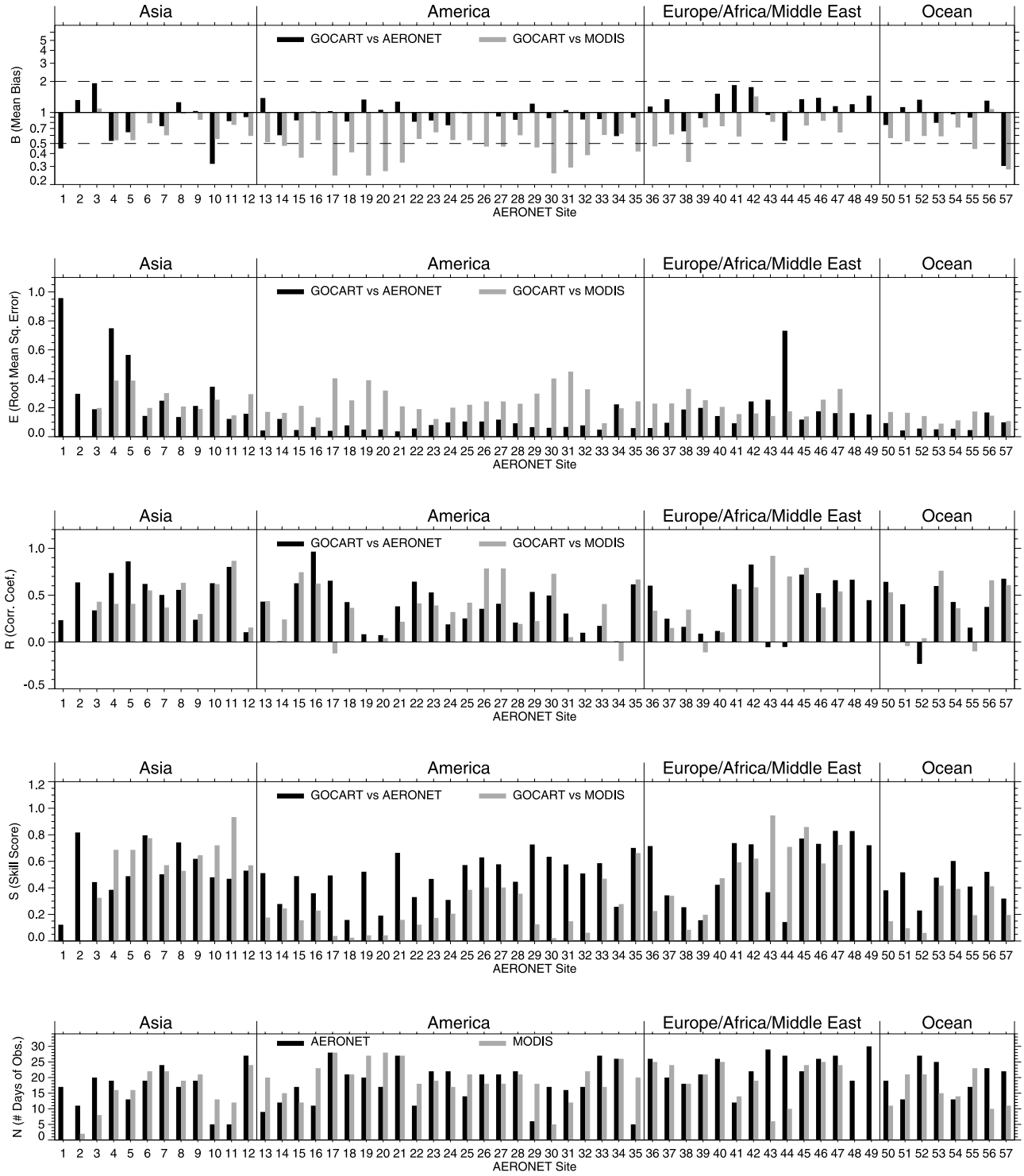

Figure 6. Mean bias B (top panel), root-mean-square error E (second panel), correlation coefficients R (third panel), and skill score S (fourth panel) between the model and AERONET (black vertical bars) or MODIS (grey vertical bars). The number of observation days in April 2001 for AERONET (black) and MODIS (grey) is shown in the bottom panel. Dashed lines in the top panel are $B = 2$ and $B = 0.5$ lines, i.e., a factor of 2 bias.

standard, the model has generally lower bias and higher correlation (except in Asia) than does MODIS. For example, the regional averaged B values of the model are 0.88, 0.89, 1.19, and 0.97 for Asia, America, Europe/Africa/Middle East, and ocean regions, respectively, as compared to 1.30, 2.13, 1.55, and 1.41 of MODIS for the same regions (Figure 8). Overall, the model shows no systematic bias against the AERONET data ($B = 0.97$) while MODIS has

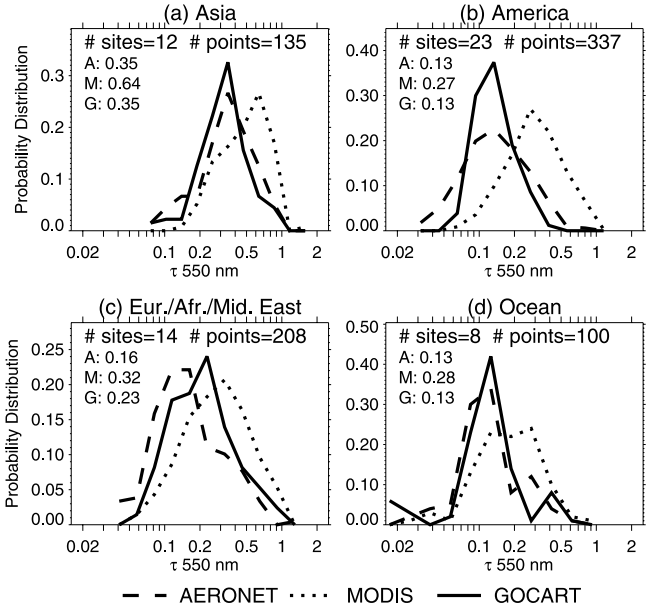

Figure 7. Probability distribution of daily τ at 550 nm in April 2001 from AERONET (dashed lines), MODIS (dotted lines), and the model (solid lines) at the AERONET sites located in (a) Asia, (b) America (North America and Surinam), (c) Europe, Africa, and Middle East, and (d) islands in the oceans. The most probable (or modal) values of AERONET (A), MODIS (M), and GOCART (G) for each region are shown in the corresponding panel.

demonstrated a high bias (B = 1.64) in the Northern Hemisphere during April 2001.

4. Aerosol Composition and Anthropogenic Component in the Northern Hemisphere During Spring 2001

[34] As we have seen in Figure 2 and Figure 5, aerosol distribution is highly inhomogeneous and its composition varies significantly from one place to another. Crucial for assessing the anthropogenic aerosol climate forcing is the knowledge of the chemical composition of the aerosol that cannot be directly measured by AERONET or MODIS, even though the fine mode fraction or size distribution plus spectral single-scattering albedo can provide useful information on anthropogenic aerosol components [e.g., *Kaufman et al.*, 2002; *Dubovik et al.*, 2002; *Christopher and Zhang*, 2004]. The model has an obvious advantage when quantifying the chemical composition and anthropogenic contributions because they are directly simulated in the model.

[35] The monthly averaged τ for April 2001 in the model, shown in Figure 4, has the highest values located near the Asian dust/pollution and African dust source regions. Figures 9a–9d depict the model-calculated percentage of the τ from sulfate, carbonaceous (OC + BC), dust, and sea-salt aerosols in April 2001. As expected, the highest percentage of each aerosol component is concentrated in its source regions (see Figure 1), especially dust which dominates in its regions (80–100% of total τ). Over land, dust and sulfate comprise the major portion (total 70–90%) of total τ over extratropical (latitudes > 30°N) regions, whereas in subtropical and tropical areas, carbonaceous aerosol or dust dominates. Carbonaceous aerosols dominate (60–90%) in southern Asia and Central America, mainly from biomass burning, whereas dust dominates (60–100%) in Africa and the Middle East. Over ocean, dust dominates the tropical/subtropical North Atlantic (40–80%), sea-salt controls the equatorial North Pacific (60–80%), and carbonaceous aerosol is the major constituent in the subtropical North Pacific and Indian Ocean (40–80%). Dust influence is also shown over a substantial area in the extratropical North Pacific and eastern North Atlantic (20–40%), with sulfate and sea salt sharing the remaining τ. We note that over the ACE-Asia experiment area in the Yellow Sea and the Sea of Japan, sulfate and dust contributes about equally to 40–50% of the total τ (Figure 9). On average, sulfate, carbon, dust, and sea salt comprise 30%, 25%, 32%, and 13% of the τ at 550 nm in April 2001 in the Northern

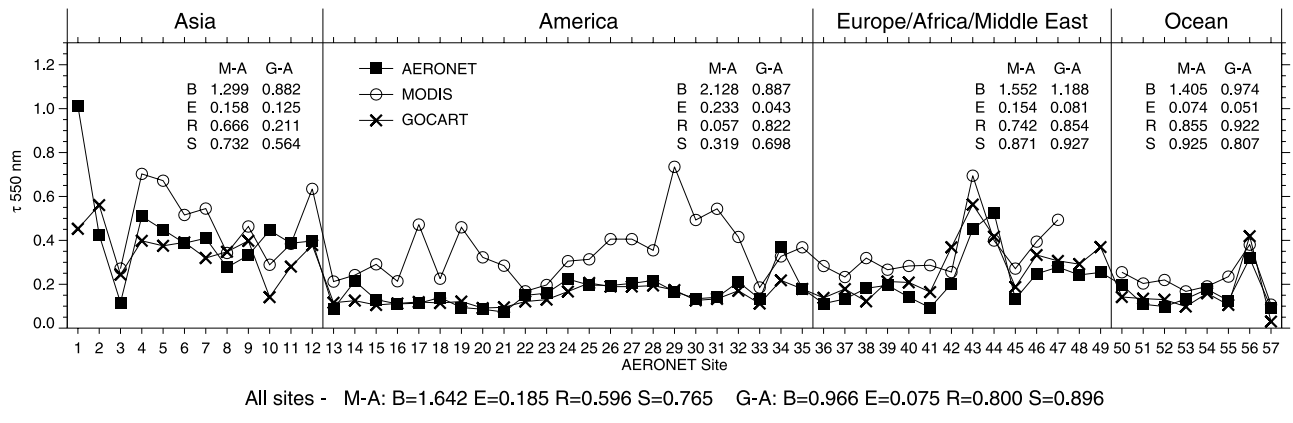

Figure 8. Monthly averaged τ at 550 nm for April 2001 at 57 AERONET sites. Data are averaged for the days when both AERONET and MODIS observations are available, except at sites 1, 2, 48, and 49, where there are no available MODIS data. Statistical parameters of mean bias B, root-mean-square error E, correlation coefficient R, and skill score S for the regions of Asia, America, Europe/Africa/Middle East, and the oceans are also listed. "M-A" is for MODIS versus AERONET, and "G-A" is for GOCART versus AERONET.

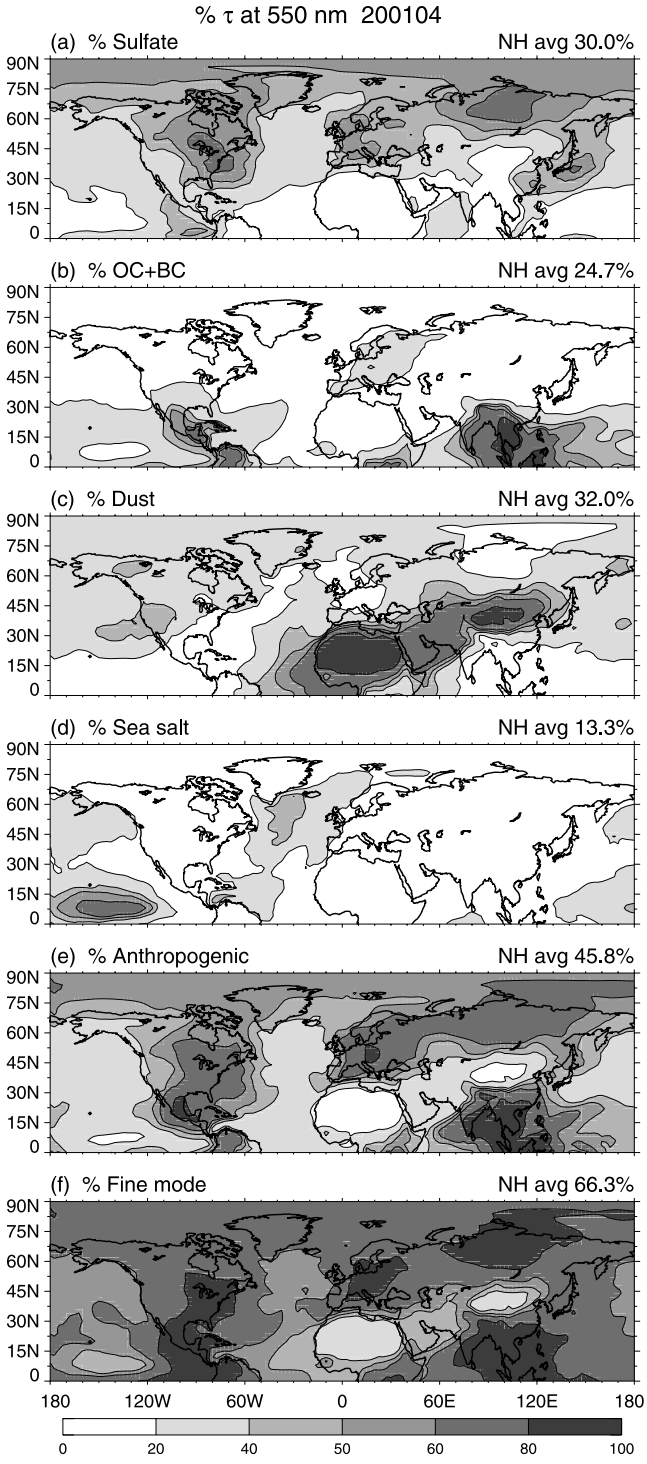

Figure 9. Model-calculated percentage contributions of (a) sulfate, (b) carbonaceous, (c) dust, (d) sea-salt, (e) anthropogenic, and (f) fine mode aerosols to the monthly averaged τ at 550 nm for April 2001 in the Northern Hemisphere.

Hemisphere. It should be pointed out that BC is optically thin, contributing to only 10–20% of τ in the tropical/subtropical regions and in central Europe, and less than 10% everywhere else. However, the low single-scattering albedo of BC makes it a very important absorbing aerosol in the atmosphere, with a significant impact on climate change [e.g., *Hansen et al.*, 2000; *Jacobson*, 2001].

[36] Figure 9e shows the anthropogenic fraction of the 550 nm τ. We define anthropogenic aerosol as the sum of sulfate, OC, and BC that are either directly emitted or chemically produced from precursors which are emitted from fossil fuel, biofuel, and biomass-burning sources; the natural aerosols are composed with dust, sea salt, and sulfate and OC that are formed from their gaseous precursors emitted from volcanoes, ocean, and vegetations. This assumption is somewhat oversimplified since, for example, not all biomass burning is human caused and some dust is "anthropogenic" emitted from desertification area caused by land use changes [e.g., *Tegen et al.*, 2004]. The model shows that anthropogenic aerosols account for more than 50% of the τ over most land areas except dust dominated regions of northern Africa, Middle East, and Asia, and western part of North America (west of 125°W). Over oceans, 20–40% of τ is of anthropogenic origin except the eastern North Atlantic and the tropical/subtropical western North Pacific and Indian oceans where anthropogenic aerosol contributes to 40–90%. The model estimates that roughly 46% of the aerosol in the Northern Hemisphere in April 2001 is anthropogenic.

[37] It is interesting to compare the anthropogenic fraction of τ with the fine mode fraction, because there have been several attempts to use the fine mode aerosol from satellite retrievals as a proxy of anthropogenic aerosol [e.g., *Kaufman et al.*, 2002; *Christopher and Zhang*, 2004]. We plot in Figure 9f the fine mode fraction in the Northern Hemisphere in April 2001 from the model. As we mentioned in section 3, the τ of fine mode aerosol from the model is the sum of values of sulfate, OC, BC, and submicron dust and sea salt. Figure 9f shows that the northern hemispheric average of fine mode aerosol τ is 66%, i.e., 20% higher than the anthropogenic τ. This is because the contributions from natural sulfate and OC aerosols (formed from oxidation of DMS, volcanic SO_2, and terpene, see section 2.1) and submicron dust and sea salt aerosols. Together, they contribute to 30% of fine mode aerosol or 20% of total aerosol.

5. Discussion

[38] The use of the MODIS and AERONET data to evaluate the model results and characterize aerosol distributions paves the way for a quantitative assessment of the regional and global consequences of pollutant and dust emissions from different areas. The global model and satellite data together can extend the limited regional ACE-Asia measurements to a much larger spatial scale.

[39] The MODIS instrument has provided aerosol products since 2000 with accuracies much higher than the products from previous satellite sensors not originally designed for measuring aerosols [*Remer et al.*, 2004]. MODIS retrieves aerosol optical depth over both land and ocean and separates it into contributions from fine and coarse modes, providing multiple parameters for evaluating global aerosol models. Yet uncertainties in the MODIS products over land are still relatively large, because of fewer usable wavelengths and much more complex surface properties than over ocean. The globally

fixed ratio of surface reflectance between the visible and infrared wavelengths (see section 2.2) used in the land retrieval may be too simple to account for the variability of the ratio for different land cover types. It is an attempt to represent the global mean of the surface reflectance correctly, but the ratio at individual locations and specific surface types will deviate from the mean. While the empirical ratio works relatively well over dark, vegetated land surfaces, it is especially difficult to deal with the land surfaces with somewhat high reflectance, such as arid regions, elevated terrain (e.g., over the Southwest United States), and snow/ice melting areas (e.g., northeast North America in the spring), as well as in the coastal or swamp areas with mixed land/water pixels [e.g., *Levy et al.*, 2004]. It is in these regions that MODIS has the largest disagreement with both AERONET and the model.

[40] One unique product derived by MODIS is the fine mode fraction of aerosols (f_τ), which can be directly related to the fraction of anthropogenic aerosol contributions to total aerosol loading, which in turn, could lead to estimates of anthropogenic climate forcing, although the model estimates that the f_τ is about 20% higher than the anthropogenic fraction in the spring time of Northern Hemisphere. The f_τ over ocean from MODIS is well defined and statistically similar to the modeled values. Over land, however, the f_τ from MODIS is rather qualitative, indicating only clear dominance of either fine or coarse aerosol (e.g., southern Asia and southern North America in Figure 3d) or a comparable mixture of both (e.g., northern Asia and northern part of North America in Figure 3d where the MODIS shows a flat distribution). Thus quantitative use of the current MODIS f_τ is, at present, only appropriate for areas over oceans. Again, the low spectral contrast from the two usable wavelengths over land, coupled with complex surface properties, leads to large uncertainties in land retrieval of f_τ. Our comparisons have shown that improvements of the MODIS land retrievals are needed. As future MODIS land aerosol retrievals will include improved screening for melting snow and other complicated land surfaces, we expect an improvement in MODIS data quality. Eventually, the MODIS land algorithm will incorporate surface reflectance ratios dependent on land cover type, which should decrease error even further.

[41] Over ocean, the MODIS and the model have shown similar distributions of τ in the extratropical oceans, but the model is usually a factor of 2 lower than the MODIS in the tropical/subtropical oceans. From the comparisons shown in Figures 6 and 8, the model seems to have relatively small mean biases against the AERONET data at 5 subtropical Pacific sites (sites 50–53 and 56, $B = 0.76 - 1.3$) where MODIS is 40–110% higher than AERONET; on the other hand, the model is a factor of 3 lower than AERONET at the tropical Indian Ocean site Male (site 57), where MODIS agrees with AERONET to within 10%. Recent studies comparing several global model results with multiple satellite products have shown that the τ values at the tropical oceans from all models are considerably lower than those from all satellite products [*Penner et al.*, 2001; *Kinne et al.*, 2003]. These studies (including this one) suffer, however, from a lack of direct measurements from AERONET and other instruments in the tropical oceans. Evidently, more direct measurements over the clean tropical/subtropical oceans are needed to help resolve the model-satellite discrepancies.

[42] The worldwide AERONET aerosol measurement data are invaluable for model evaluations. Because AERONET represents most major aerosol regimes around the globe, the data are very helpful for statistical evaluations. Although the AERONET data are "point" measurements that are not necessarily representative of the 2° grid model results, the daily averaged data should be relatively unbiased. The spatial inhomogeneity in the 2° model grid should be much reduced by the time averaging, except near emission sources that have very large spatial and temporal variations. Even though we have shown that the model successfully reproduces aircraft measured dust concentrations downwind of the Yellow Sea and the Sea of Japan [*Chin et al.*, 2003], the dust τ from the model is different by a factor of 2 as compared to AERONET valued in the Asian dust source region (one-half Dunhuang but double in Dalanzadgad). This discrepancy reflects not only the difficulties in simulating inhomogenous dust at the source by a relatively coarse resolution model, but also the need to improve the dust emission parameters within the model. For regions where aerosol emission is relatively constant and well known, such as North America, the model simulations are quite accurate and can be used quantitatively.

[43] The AERONET data are very useful in evaluating errors and biases in both the satellite and the model products. These direct measurement data can help improve the satellite retrieval algorithms and the model's physical processes, and resolve discrepancies between their corresponding products. Although the comparison between the $1° \times 1°$ gridded MODIS retrieval and the daytime averaged AERONET data is not optimal for satellite data validation (the MODIS validation has been performed using the 10-km resolution data [e.g., *Remer et al.*, 2004]), the persistent high bias of MODIS retrieval over some land regions shown in this study is beyond the issue of resolution comparability. Instead, it reflects a general difficulty in MODIS land retrieval. This is highly relevant to some recent "aerosol assimilation" efforts that integrate satellite products with global model simulations to better describe the global aerosol distributions [e.g., *Collins et al.*, 2001; *Yu et al.*, 2003]. We argue that the AERONET data should be an important part in generating such integrated products, in order to reduce large errors or biases in the satellite retrievals or model results in the integrated system. This is especially appropriate over surfaces that have complicated physical and optical properties.

[44] We have emphasized the use of statistical parameters to quantitatively address the degree of agreement between the model and data. The quantitative evaluation is particularly important when a model is used to estimate unavailable or immeasurable quantities (e.g., anthropogenic contributions and intercontinental transport fluxes) and to project future atmospheric changes. "Eyeball" verifications that look the model and data side by side are valid for demonstrations and qualitative judgment, but they are subject to individual interpretations and are not quantitative, while as shown in this study a few statistical parameters (e.g., *HERBS*) generate much more effective and insightful evaluations. While similarities and differences are compounded in the skill scores, they are revealed individually

in the bias, error, and correlation analysis. Given the differences in the spatial and temporal resolutions among AERONET, MODIS, and the GOCART model that make point-by-point comparisons uncertain, histogram is especially appropriate in assessing the behavior of each data set on a common ground. Our more extensive comparisons and analyses of the AERONET, MODIS, and the model including other seasons and the Southern Hemisphere are currently underway for a more comprehensive assessment.

6. Conclusions

[45] We have compared the GOCART model simulated aerosol optical thickness τ at 550 nm with the AERONET Sun photometer data and the MODIS satellite retrievals for the ACE-Asia period of April 2001. These comparisons are made not only for the dust and pollution source regions in Asia and its immediate downwind regions, which comprised the ACE-Asia measurement area, but also for other regions of North/South America, Europe, Africa, Middle East, and oceans in the Northern Hemisphere that are connected by long-range transport. This exercise has produced a quantitative assessment of the model's performance and credibility in estimating the impact of aerosols originating from different source regions on the global atmosphere.

[46] We have used a set of statistical parameters, including histograms H, root-mean-square error E, correlation coefficient R, mean bias B, and skill scores S (*HERBS*), to evaluate the model and quantify the similarities and differences between the data sets and the model results. We have shown that these statistical parameters can provide effective and insightful evaluations, which are especially helpful when the differences in the spatial and temporal resolutions among different data sets make point-by-point comparisons uncertain. We recommend that these statistical methods be more widely used in model evaluation, data validation, and in the intercomparisons of models and data.

[47] Both MODIS and the model have shown relatively high τ near the source regions such as eastern Asia, Europe, and northern Africa, and are consistent regarding the major features of the long-range transport of aerosols from their source regions to the neighboring oceans. The probability distributions (or normalized histograms) between the τ values from MODIS and from the model are very similar for the northern part (north of 30°N) of the oceans, but they are a factor of 2 apart for the tropical/subtropical oceans (model being lower). Over land, the distributions of τ from the MODIS and the model are very similar over Europe, but the model is considerably lower than the MODIS in other land regions, especially over North America where model is a factor of 2–3 lower than the MODIS. Comparisons with the AERONET measurements have demonstrated that in general the model and AERONET have comparable values and similar probability distributions of τ, but MODIS has a high bias especially in America (greater than a factor of 2), which is largely attributed to the difficulties in the MODIS retrieval dealing with the high surface reflectance at the mountaintop, arid areas, and snow/ice melting places during the spring. Further improvements of the MODIS land retrieval that applies a more rigorous snow/ice mask and deals more effectively with land-cover-type-dependent surface reflectance are needed to reduce the bias. The discrepancy in the tropical/subtropical regions remains to be resolved, as the comparisons with a few available AERONET sites in this region are still inconclusive, although it is possible that the model has underestimated the sources or overestimated the sinks in the tropics. Since such discrepancy is common between global models and satellite data, more direct measurements focusing on the tropical/subtropical regions are needed. In general, the model has shown no systematic bias against the AERONET data whereas the MODIS is about 60% too high compared to AERONET in spring 2001.

[48] We have applied the model results to estimate the composition of aerosols in spring 2001 and the anthropogenic contributions. On average, sulfate, carbon, dust, and sea salt comprise 30%, 25%, 32%, and 13%, respectively, of the 550-nm τ in April 2001 in the Northern Hemisphere. Over land, dust and sulfate are the major contributors to the total τ in the extratropical region, while carbonaceous aerosol is the most significant component over the subtropical and tropical area in southern Asia and Central America, mainly from biomass burning. Over oceans, dust dominates the tropical/subtropical North Atlantic, sea-salt controls the equatorial North Pacific, and carbonaceous aerosol affects the subtropical North Pacific and Indian Ocean. Dust also influences a substantial area in the extratropical North Pacific and North Atlantic. The model estimates that anthropogenic aerosols contribute, on average, nearly 46% to the τ at 550 nm in the Northern Hemisphere in April 2001. Anthropogenic activities account for more than 50% of the τ over substantial land areas in Asia, North/Central America, Europe and Eurasia, and subtropical western North Pacific and Indian oceans, and 20–40% over the rest of the oceans. Although the fine mode aerosol fractions retrieved from MODIS can potentially be used to derive information on anthropogenic contributions, the model shows that on average the τ at 550 nm from fine mode aerosol is about 20% higher than that from anthropogenic aerosols in the Northern Hemisphere during April 2001, because of the natural sources of sulfate and OC and the submicron dust and sea salt that contribute to 30% of total fine mode aerosols.

[49] **Acknowledgments.** This work was supported by the NASA Atmospheric Composition Modeling and Analyis Program (ACMAP) and Radiation Science Program (RSP). We thank Colette Heald for providing the biomass-burning emission inventory for spring 2001 and the principal investigators and field managers of the AERONET sites and the AERONET program team for providing the Sun photometer data used in this work. The comments from two anonymous reviewers are deeply appreciated. This research is a contribution to the International Global Atmospheric Chemistry (IGAC) Core project of the International Geosphere Biosphere Program (IGBP) and is part of the IGAC Aerosol Characterization Experiments (ACE).

References

Chin, M., R. B. Rood, S.-J. Lin, J.-F. Müller, and A. M. Thomspon (2000a), Atmospheric sulfur cycle in the global model GOCART: Model description and global properties, *J. Geophys. Res.*, *105*, 24,661–24,687.

Chin, M., D. Savoie, B. J. Huebert, A. R. Bandy, D. C. Thornton, T. S. Bates, P. K. Quinn, E. S. Saltsman, and W. J. De Bruyn (2000b), Atmospheric sulfur cycle in the global model GOCART: Comparison with field observations and regional budgets, *J. Geophys. Res.*, *105*, 24,689–24,712.

Chin, M., P. Ginoux, S. Kinne, O. Torres, B. N. Holben, B. N. Duncan, R. V. Martin, J. A. Logan, A. Higurashi, and T. Nakajima (2002), Tropospheric aerosol optical thickness from the GOCART model and comparisons with satellite and sunphotometer measurements, *J. Atmos. Sci.*, *59*, 461–483.

Chin, M., P. Ginoux, R. Lucchesi, B. Huebert, R. Weber, T. Anderson, S. Masonis, B. Blomquist, A. Bandy, and D. Thornton (2003), A global aerosol model forecast for the ACE-Asia field experiment, *J. Geophys. Res.*, *108*(D23), 8654, doi:10.1029/2003JD003642.

Christopher, S. A., and J. Zhang (2004), Cloud-free shortwave aerosol radiative effect over oceans: Strategies for identifiying anthropogenic forcing from Terra satellite measurements, *Geophys. Res. Lett.*, *31*, L18101, doi:10.1029/2004GL020510.

Chu, D. A., Y. J. Kaufman, L. A. Remer, D. Tanré, and B. N. Holben (1998), Remote sensing of smoke from MODIS airborne simulator during the SCAR-B experiment, *J. Geophys. Res.*, *103*, 31,979–31,988.

Chu, D. A., Y. J. Kaufman, C. Ichoku, L. A. Remer, D. Tanré, and B. N. Holben (2002), Validation of MODIS aerosol optical depth retrieval over land, *Geophys. Res. Lett.*, *29*(12), 8007, doi:10.1029/2001GL013205.

Chu, D. A., Y. J. Kaufman, G. Zibordi, J. D. Chern, J. Mao, C. Li, and B. N. Holben (2003), Global monitoring of air pollution over land from the Earth Observing System-Terra Moderate Resolution Imaging Spectroradiometer (MODIS), *J. Geophys. Res.*, *108*(D21), 4661, doi:10.1029/2002JD003179.

Collins, W. D., P. J. Rasch, B. E. Eaton, B. V. Khattatov, J.-F. Lamarque, and C. S. Zender (2001), Simulating aerosols using a chemical transport model with assimilation of satellite aerosol retrievals: Methodology for INDOEX, *J. Geophys. Res.*, *106*, 7313–7336.

Dubovik, O., B. N. Holben, T. F. Eck, A. Smirnov, Y. J. Kaufman, M. D. King, D. Tanré, and I. Slutsker (2002), Variability of absorption and optical properties of key aerosol types observed in worldwide locations, *J. Atmos. Sci.*, *59*, 590–608.

Duncan, B. N., R. V. Martin, A. C. Staudt, R. Yevich, and J. A. Logan (2003), Interannual and seasonal variability of biomass burning emissions constrained by satellite observations, *J. Geophys. Res.*, *108*(D2), 4100, doi:10.1029/2002JD002378.

Eck, T. F., B. N. Holben, J. S. Reid, O. Dubovik, A. Smirnov, N. T. O'Neill, I. Slutsker, and S. Kinne (1999), Wavelength dependence of the optical depth of biomass burning, urban and desert dust aerosols, *J. Geophys. Res.*, *104*, 31,333–31,350.

Ginoux, P., M. Chin, I. Tegen, J. Prospero, B. Holben, O. Dubovik, and S.-J. Lin (2001), Sources and global distributions of dust aerosols simulated with the GOCART model, *J. Geophys. Res.*, *106*, 20,255–20,273.

Ginoux, P., J. Prospero, O. Torres, and M. Chin (2004), Long-term simulation of dust distribution with the GOCART model: Correlation with the North Atlantic Oscillation, *Environ. Model. Software*, *19*, 113–128.

Hansen, J., M. Sato, R. Ruedy, A. Lacis, and V. Oinas (2000), Global warming in the twenty-first century: An alternative scenario, *Proc. Natl. Acad. Sci. U. S. A.*, *97*, 9800–9875.

Heald, C. L., D. J. Jacob, P. I. Palmer, M. J. Evans, G. W. Sachse, H. B. Singh, and D. J. Blake (2003), Biomass burning emission inventory with daily resolution: Application to aircraft observations of Asian outflow, *J. Geophys. Res.*, *108*(D21), 8811, doi:10.1029/2002JD003082.

Holben, B. N., et al. (1998), AERONET: A federated instrument network and data archive for aerosol characterization, *Remote Sens. Environ.*, *66*, 1–16.

Holben, B. N., et al. (2001), An emerging ground-based aerosol climatology: Aerosol optical depth from AERONET, *J. Geophys. Res.*, *106*, 12,067–12,097.

Huebert, B., T. Bates, P. B. Russell, G. Shi, Y. J. Kim, K. Kawamura, G. Carmichael, and T. Nakajima (2003), An overview of ACE-Asia: Strategies for quantifying the relationships between Asian aerosols and their climate impacts, *J. Geophys. Res.*, *108*(D23), 8633, doi:10.1029/2003JD003550.

Jacobson, M. Z. (2001), Strong radiative heating due to the mixing state of black carbon in atmospheric aerosols, *Nature*, *409*, 695–697.

Kaufman, Y. J., D. Tanré, L. A. Remer, E. Vermote, A. Chu, and B. N. Holben (1997a), Operational remote sensing of tropospheric aerosol over the land from EOS Moderate Resolution Imaging Spectroradiometer, *J. Geophys. Res.*, *102*, 17,015–17,061.

Kaufman, Y. J., A. Wald, L. A. Remer, B.-C. Gao, R.-R. Li, and L. Flynn (1997b), The MODIS 2.1 μm channel-correlation with visible reflectance for use in remote sensing of aerosol, *IEEE Trans. Geosci. Remote Sens.*, *35*, 1286–1298.

Kaufman, Y. J., D. Tanré, and O. Boucher (2002), A satellite view of aerosols in the climate system, *Nature*, *419*, 215–223.

King, M. D., J. Y. Kaufman, D. Tanré, and T. Nakajima (1999), Remote sensing of tropospheric aerosols from space: Past, present, and future, *Bull. Am. Meteorol. Soc.*, *80*, 2229–2259.

Kinne, S., et al. (2003), Monthly averages of aerosol properties: A global comparison among models, satellite data, and AERONET ground data, *J. Geophys. Res.*, *108*(D20), 4634, doi:10.1029/2001JD001253.

Lesins, G., P. Chylek, and U. Lohmann (2002), A study of internal and external mixing scenarios and its effect on aerosol optical properties and direct radiative forcing, *J. Geophys. Res.*, *107*(D10), 4094, doi:10.1029/2001JD000973.

Levy, R. C., L. A. Remer, D. Tanré, Y. J. Kaufman, C. Ichoku, B. N. Holben, J. M. Livingston, P. B. Russell, and H. Maring (2003), Evaluation of the Moderate-Resolution Imaging Spectroradiometer (MODIS) retrievals of dust aerosol over the ocean during PRIDE, *J. Geophys. Res.*, *108*(D19), 8594, doi:10.1029/2002JD002460.

Levy, R. C., L. A. Remer, J. V. Martins, Y. J. Kaufman, A. Plana-Fattori, J. Redemann, P. B. Russell, and B. Wenny (2004), Evaluation of the MODIS aerosol retrievals over ocean and land during CLAMS, *J. Atmos. Sci*, in press.

Nakićenović, N., et al. (2000), *Emissions Scenarios: A Special Report of Working Group III of the Intergovernmental Panel on Climate Change*, 599 pp., Cambridge Univ. Press, New York.

O'Neill, N. T., A. Ignatov, B. N. Holben, and T. F. Eck (2000), The log-normal distribution as a reference for reporting aerosol optical depth statistics; Empirical tests using multi-year, multi-site AERONET sunphotometer data, *Geophys. Res. Lett.*, *27*, 3333–3336.

Penner, J. S., et al. (2001), Aerosols, their direct and indirect effects, in *Climate Change 2001: The Scientific Basis, Contribution of Working Group I to the Third Assessment Report of the Intergovernmental Panel on Climate Change*, edited by J. T. Houghton et al., chap. 5, pp. 289–348, Cambridge Univ. Press, New York.

Remer, L. A., et al. (2002), Validation of MODIS aerosol retrieval over ocean, *Geophys. Res. Lett.*, *29*(12), 8008, doi:10.1029/2001GL013204.

Remer, L. A., et al. (2004), The MODIS aerosol algorithm, products and validation, *J. Atmos. Sci.*, in press.

Smirnov, A., B. N. Holben, T. F. Eck, O. Dubovik, and I. Slutsker (2000), Cloud screening and quality control algorithms for the AERONET database, *Remote Sens. Environ.*, *73*, 337–349.

Streets, D., et al. (2003), An inventory of gaseous and primary aerosol emissions in Asia in the year 2000, *J. Geophys. Res.*, *108*(D21), 8809, doi:10.1029/2002JD003093.

Tanré, D., Y. J. Kaufman, M. Herman, and S. Mattoo (1997), Remote sensing of aerosol properties over oceans using the MODIS/EOS spectral radiances, *J. Geophys. Res.*, *102*, 16,971–16,988.

Taylor, K. E. (2001), Summarizing multiple aspects of model performance in a single diagram, *J. Geophys. Res.*, *106*, 7183–7192.

Tegen, I., M. Werner, S. P. Harrison, and K. E. Kohfeld (2004), Relative importance of climate and land use in determining present and future global soil dust emission, *Geophys. Res. Lett.*, *31*, L05105, doi:10.1029/2003GL019216.

Yu, H., R. E. Dickinson, M. Chin, Y. J. Kaufman, B. N. Holben, I. V. Geogdzhayev, and M. I. Mishchenko (2003), Annual cycle of global distribution of aerosol optical depth from integration of MODIS retrievals and GOCART model simulations, *J. Geophys. Res.*, *108*(D3), 4128, doi:10.1029/2002JD002717.

M. Chin, A. Chu, Y. Kaufman, R. Levy, and L. Remer, Laboratory for Atmospheres, NASA Goddard Space Flight Center, M. S. 916.0, Building 21, Room C217, Greenbelt, MD 20771, USA. (mian.chin@nasa.gov; achu@crb02.gsfc.nasa.gov; kaufman@climate.gsfc.nasa.gov; levy@climate.nasa.gov; remer@climate.gsfc.nasa.gov)

T. Eck and B. Holben, Laboratory for Terrestrial Physics, NASA Goddard Space Flight Center, Code 923, Greenbelt, MD 20771, USA. (tom@aeronet.gsfc.nasa.gov; brent@aeronet.gsfc.nasa.gov)

Q. Gao, Chinese Academy of Environmental Science, 8 Dayangfang, Andingmenwai, Beijing 100012, China. (gaoqx@creas.org.cn)

P. Ginoux, NOAA Geophysical Fluid Dynamics Laboratory, Forrestal Campus, Route 1, P. O. Box 308, Princeton, NJ 08542, USA. (paul.ginoux@noaa.gov)